1

Introduction: mesoscopic physics

1.1 Interference and disorder

Wave propagation in a random medium is a phenomenon common to many areas of physics. There has been a recent resurgence of interest following the discovery, in both optics and quantum mechanics, of surprising coherent effects in a regime in which disorder was thought to be sufficiently strong to eliminate a priori all interference effects.

To understand the origin of these coherent effects, it may be useful to recall some general facts about interference. Although quite spectacular in quantum mechanics, their description is more intuitive in the context of physical optics. For this reason, we begin with a discussion of interference effects in optics.

Consider a monochromatic wave scattered by an obstacle of some given geometry, e.g., a circular aperture. Figure 1.1 shows the diffraction pattern on a screen placed infinitely far from the obstacle. It exhibits a set of concentric rings, alternately bright and dark, resulting from constructive or destructive interference. According to Huygens' principle, the intensity at a point on the screen may be described by replacing the aperture by an ensemble of virtual coherent point sources and considering the difference in optical paths associated with these sources. In this way, it is possible to associate each interference ring with an integer (the equivalent of a quantum number in quantum mechanics).

Let us consider the robustness of this diffraction pattern. If we illuminate the obstacle by an incoherent source for which the length of the emitted wave trains is sufficiently short that the different virtual sources are out of phase, then the interference pattern on the screen will disappear and the screen will be uniformly illuminated. Contrast this with the following situation: employ a coherent light source and rapidly move the obstacle in its plane in a random fashion. Here too, the interference fringes are replaced by uniform illumination. In this case, it is the persistence of the observer's retina that averages over many different displaced diffraction patterns. This example illustrates two ways in which the diffraction pattern can disappear. In the former case, the disappearance is associated with a random distribution of the lengths of wave trains emanating from the source, while in the latter case, it is the result of an *average* over an ensemble of spatially distributed virtual sources. This example shows how interference effects may vanish upon averaging.

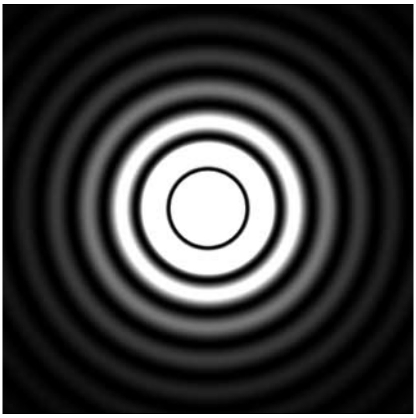

Figure 1.1 Diffraction pattern at infinity for a circular aperture.

Let us now turn to the diffraction of a coherent source by an obstacle of arbitrary type. For instance, suppose that the obstacle is a dielectric material whose refractive index fluctuates in space on a scale comparable to the wavelength of the light. The resulting scattering pattern on a screen placed at infinity, consists of a random distribution of bright and dark areas, as seen in Figure 1.2; this is called a *speckle* pattern.[1] Each speckle associated with the scattering represents a *fingerprint* of the random obstacle, and is specific to it. However, in contrast to the case of scattering by a sufficiently symmetric obstacle (such as a simple circular aperture), it is impossible to identify an order in the speckle pattern, and thus we cannot describe it with a deterministic sequence of integer numbers. This impossibility is one of the characteristics of what are termed complex media.

In this last experiment, for a thin enough obstacle, a wave scatters only once in the random medium before it emerges on its way to the screen at infinity (see Figure 1.3(a)). This regime is called *single scattering*. Consider now the opposite limit of an optically thick medium (also called a turbid medium), in which the wave scatters many times before leaving (Figure 1.3(b)). We thus speak of *multiple scattering*. The intensity at a point on the screen is obtained from the sum of the complex amplitudes of the waves arriving at that point. The phase associated with each amplitude is proportional to the path length of the multiply scattered wave divided by its wavelength λ. The path lengths are randomly distributed, so one would expect that the associated phases fluctuate and average to zero. Thus, the total intensity would reduce to the sum of the intensities associated with each of the paths.

In other words, if we represent this situation as equivalent to a series of thin obstacles, with each element of the series corresponding to a different and independent realization of the random medium, we might expect that for a sufficiently large number of such thin

[1] These speckles resemble those observed with light emitted by a weakly coherent laser, but they are of a different nature. Here they result from static spatial fluctuations due to the inhomogeneity of the scattering medium.

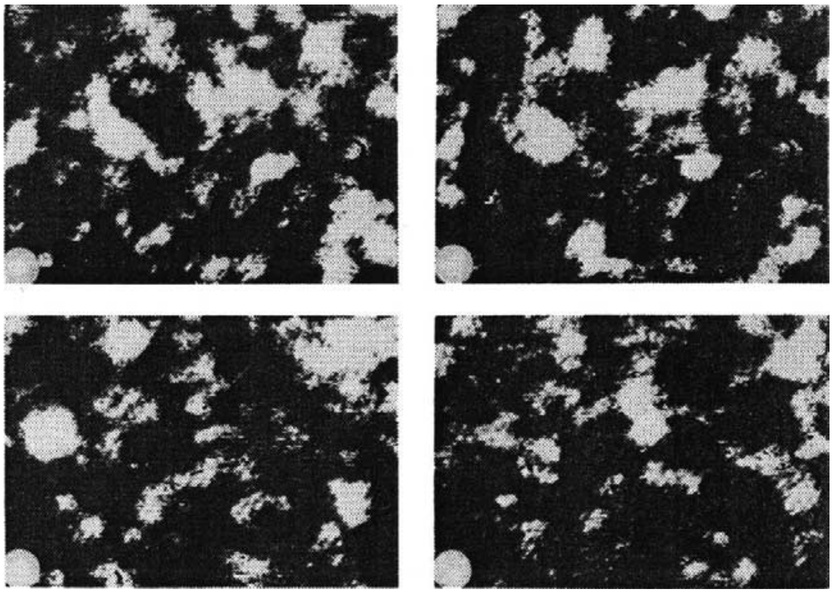

Figure 1.2 Speckle patterns due to scattering through an inhomogeneous medium. Here the medium is optically thick, meaning that the incident radiation undergoes many scatterings before leaving the sample. Each image corresponds to a different realization of the random medium [1].

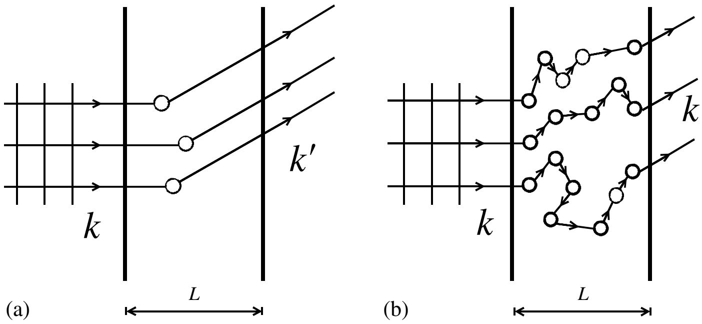

Figure 1.3 Schematic representations of the regimes of (a) single scattering, and (b) multiple scattering.

obstacles, the resulting intensity at a point on the screen would average over the different realizations, causing the speckles to vanish. This point of view corresponds to the classical description, for which the underlying wave nature plays no further role.

Figures 1.2 and 1.4 show that this conclusion is incorrect, and that the speckles survive, *even in the regime of multiple scattering*. If, on the other hand, we perform an ensemble

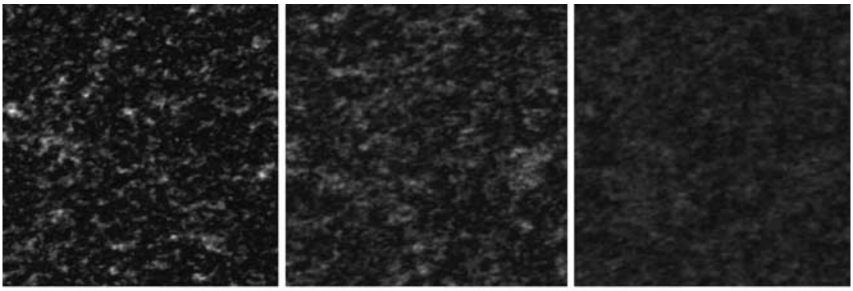

Figure 1.4 Averaging. The first speckle pattern (a) represents a snapshot of a random medium corresponding to a single realization of the disorder. The other two figures (b and c) correspond to an integration over the motion of scatterers, and hence to a self-average. (Figure courtesy of Georg Maret.)

average, the diffraction pattern disappears. This is the case with turbid media such as the atmosphere or suspensions of scatterers in a liquid (milk, for example), where the motion of the scatterers yields an average over different realizations of the random medium, provided we wait long enough. The classical approach, therefore, correctly describes the average characteristics of a turbid medium, such as the transmission coefficient or the diffusion coefficient of the average intensity. It has been employed extensively in problems involving the radiative transfer of waves through the atmosphere or through turbulent media.

This description may be adapted as such to the problem of propagation of electrons in a metal. In this case, the impurities in the metal are analogous to the scatterers in the optically thick medium, and the quantity analogous to the intensity is the electrical conductivity. In principle, of course, it is necessary to use the machinery of quantum mechanics to calculate the electrical conductivity. But since the work of Drude at the beginning of the last century, it has been accepted that transport properties of metals are correctly described by the disorder-averaged conductivity, obtained from a classical description of the degenerate electron gas. However, for a given sample, i.e., for a specific realization of disorder, we may observe interference effects, which only disappear upon averaging [2].

The indisputable success of the classical approach led to the belief that coherent effects would not subsist in a random medium in which a wave undergoes multiple scattering. In the 1980s, however, a series of novel experiments unequivocally proved this view to be false. In order to probe interference effects, we now turn to the Aharonov–Bohm effect, which occurs in the most spectacular of these experiments.

1.2 The Aharonov–Bohm effect

The Young two-slit device surely provides the simplest example of an interference pattern in optics; understanding its analog in the case of electrons is necessary for understanding quantum interference effects. In the Aharonov–Bohm geometry, an infinite solenoid is

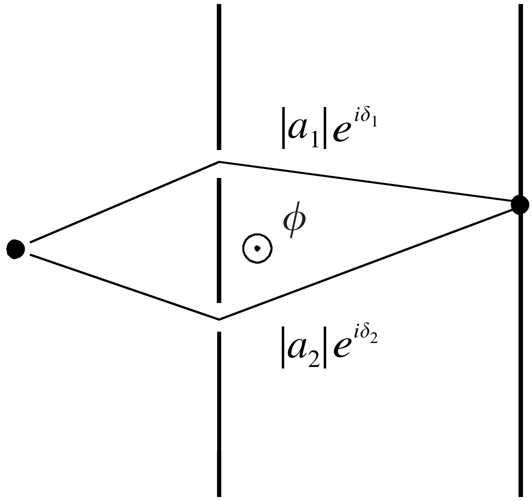

Figure 1.5 Schematic representation of the Aharonov–Bohm effect. A flux tube of flux ϕ is placed behind the two slits.

placed between the slits, such that the paths of the interfering electrons are exterior to it, as indicated in Figure 1.5. The magnetic field outside the solenoid is zero, so that classically it has no effect on the motion of the electrons.

This is not the case in quantum mechanics where, to calculate the intensity, we must sum the complex amplitudes associated with different trajectories. For the two trajectories of Figure 1.5, the amplitudes have the form $a_{1,2} = |a_{1,2}|e^{i\delta_{1,2}}$, where the phases δ_1 and δ_2 are given by ($-e$ is the electron charge):

$$\begin{aligned} \delta_1 &= \delta_1^{(0)} - \frac{e}{\hbar}\int_1 \boldsymbol{A}\cdot d\boldsymbol{l} \\ \delta_2 &= \delta_2^{(0)} - \frac{e}{\hbar}\int_2 \boldsymbol{A}\cdot d\boldsymbol{l}. \end{aligned} \tag{1.1}$$

The integrals are the line integrals of the vector potential $\boldsymbol{A}$ along the two trajectories and $\delta_{1,2}^{(0)}$ are the phases in the absence of magnetic flux. In the presence of a magnetic flux ϕ induced by the solenoid, the intensity $I(\phi)$ is given by

$$\begin{aligned} I(\phi) &= |a_1 + a_2|^2 = |a_1|^2 + |a_2|^2 + 2|a_1 a_2|\cos(\delta_1 - \delta_2) \\ &= I_1 + I_2 + 2\sqrt{I_1 I_2}\cos(\delta_1 - \delta_2). \end{aligned} \tag{1.2}$$

The phase difference $\Delta\delta(\phi) = \delta_1 - \delta_2$ between the two trajectories is now modulated by the magnetic flux ϕ

$$\Delta\delta(\phi) = \delta_1^{(0)} - \delta_2^{(0)} + \frac{e}{\hbar}\oint \boldsymbol{A}\cdot d\boldsymbol{l} = \Delta\delta^{(0)} + 2\pi\frac{\phi}{\phi_0}, \tag{1.3}$$

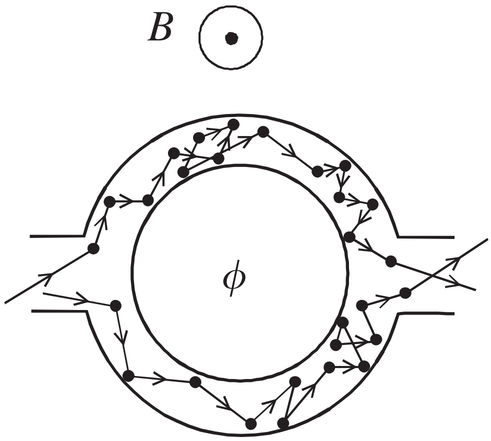

Figure 1.6 Schematic description of the experiment of Webb *et al.* on the Aharonov–Bohm effect in a metal. In this experiment, the applied magnetic field is uniform. ϕ is the flux through the ring.

where $\phi_0 = h/e$ is the quantum of magnetic flux. It is thus possible to vary continuously the state of interference at each point on the screen by changing the magnetic flux ϕ. This is the *Aharonov–Bohm effect* [3]. It is a remarkable probe to study phase coherence in electronic systems [4]. This constitutes an advantage for electronic systems over their optical counterparts.[2]

This effect was observed in the following experiment. A coherent stream of electrons was emitted by an electron microscope and split in two before passing through a toroidal magnet whose magnetic field was confined to the inside of the torus [6]. Thus, the magnetic field was zero along the trajectories of electrons. However, this experiment was performed in vacuum, where the electrons do not undergo any scattering before interfering. In order to demonstrate possible phase coherence in metals, in which the electrons undergo many collisions, R. Webb and his collaborators (1983) measured the resistance of a gold ring [7]. In the setup depicted schematically in Figure 1.6, electrons are constrained to pass through the two halves of the ring, which are analogous to the two Young slits, before being collected at the other end.

The analog of the intensity $I(\phi)$ is the electrical current, or better yet, the conductance $G(\phi)$ measured for different values of the magnetic flux ϕ. The flux is produced by applying a uniform magnetic field, though this does not strictly correspond to the Aharonov–Bohm experiment, since the magnetic field is not zero along the trajectories of electrons. However, the applied field is sufficiently weak that firstly, there is no deflection of the trajectories due to the Lorentz force, and secondly, the dephasing of coherent trajectories due to the magnetic field is negligible in the interior of the ring. Thus, the effect of the magnetic field may be neglected in comparison to that of the flux. Figure 1.7 shows that the magnetoresistance

[2] In a rotating frame, there is an analogous effect, called the Sagnac effect [5].

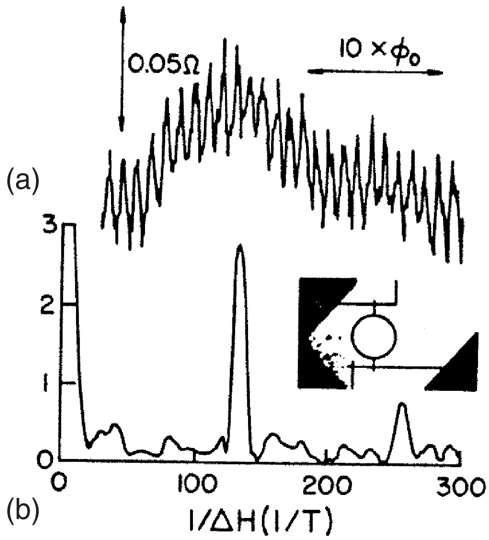

Figure 1.7 (a) Magnetoresistance of a gold ring at low temperature $T = 0.01$ K, (b) Fourier spectrum of the magnetoresistance. The principal contribution is that of the Fourier component at $\phi_0 = h/e$ [7].

of this ring is, to first approximation, a periodic function of the applied flux whose period is the flux quantum $\phi_0 = h/e$. Indeed, since the relative phase of the two trajectories is modulated by the flux, the total current, and therefore the conductance of the ring, are periodic functions of the flux:[3]

$$G(\phi) = G_0 + \delta G \cos\left(\Delta\delta^{(0)} + 2\pi \frac{\phi}{\phi_0}\right). \tag{1.4}$$

This modulation of the conductance as a function of flux results from the existence of *coherent effects* in a medium in which the disorder is strong enough for electrons to be *multiply scattered*. Consequently, the naive argument that phase coherence disappears in this regime is incorrect, and must be reexamined.

1.3 Phase coherence and the effect of disorder

In the aforementioned experiment of Webb *et al.*, the size of the ring was of the order of a micrometer. Now we know that for a macroscopic system, the modulation as a function of magnetic flux disappears. Therefore, there exists a characteristic length such that on

[3] We see in Figure 1.7 that the modulation is not purely periodic. This is due to the fact that the ring is not one dimensional. Moreover, multiple scattering trajectories within the same branch may also be modulated by the magnetic field which penetrates into the ring itself. This is the origin of the low-frequency peak in Figure 1.7(b).

scales greater than this length, there is no longer any phase coherence. This length, called the *phase coherence length* and denoted L_ϕ, plays an essential role in the description of coherent effects in complex systems.

In order to understand better the nature of this length, it is useful to review some notions related to quantum coherence.[4] Consider an ensemble of quantum particles contained in a cubic box of side length L in d dimensions. The possible quantum states are coherent superpositions of wave-functions such that the quantum state of the system is coherent over the whole volume L^d. There are many examples in which quantum coherence extends up to the macroscopic scale: superconductivity, superfluidity, free electron gas at zero temperature, coherent states of the photon field, etc.

For the electron gas at finite temperature, this coherence disappears at the macroscopic scale. It is therefore possible to treat physical phenomena such as electrical or thermal transport, employing an essentially classical approach. The suppression of quantum coherence results from phenomena linked to the existence of incoherent and irreversible processes due to the coupling of electrons to their environment. This environment consists of degrees of freedom with which the electrons interact: thermal excitations of the atomic lattice (phonons), impurities having internal degrees of freedom, interaction with other electrons, etc. This irreversibility is a source of decoherence for the electrons and its description is a difficult problem which we shall consider in Chapters 6 and 13. The phase coherence length L_ϕ generically describes the loss of phase coherence due to irreversible processes. In metals, the phase coherence length is a decreasing function of temperature. In practice, L_ϕ is of the order of a few micrometers for temperatures less than one kelvin.

None of the above considerations are related to the existence of *static* disorder of the type discussed in the two previous sections (e.g., static impurities such as vacancies or substitutional disorder, or variation of the refractive index in optics). Such disorder *does not destroy the phase coherence* and does not introduce any irreversibility. However, the possible symmetries of the quantum system disappear in such a way that it is no longer possible to describe the system with quantum numbers. In consequence, each observable of a random medium depends on the specific distribution of the disordered potential. On average, it is possible to characterize the disorder by means of a characteristic length: the *elastic mean free path* l_e, which represents the average distance travelled by a wave packet between two scattering events with no energy change (see Chapters 3 and 4).

We see, therefore, that the phase coherence length L_ϕ is fundamentally different from the elastic mean free path l_e. For sufficiently low temperatures, these two lengths may differ by several orders of magnitude, so that an electron may propagate in a disordered medium a distance much larger than l_e keeping its phase coherence, so long as the length of its trajectory does not exceed L_ϕ. The loss of coherence, therefore, is not related to the existence of a random potential of any strength, but rather to other types of mechanisms. It may seem surprising that the distinction between the effect of elastic disorder described by l_e and

[4] Most of the notions discussed here use the language of quantum mechanics; however, they have more or less direct analogs in the case of electromagnetic wave propagation.

that associated with irreversible processes of phase relaxation was first demonstrated in the relatively non-trivial case of transport in a metal where the electrons have complex interactions with their environment. However, the same distinction also applies to electromagnetic wave propagation in turbid media in the regime of coherent multiple scattering.

1.4 Average coherence and multiple scattering

If phase coherence leads to interference effects for a specific realization of disorder, it might be thought that these would disappear upon averaging. In the experiment of Webb *et al.* described in section 1.2, the conductance oscillations of period $\phi_0 = h/e$ correspond to a specific ring. If we now average over disorder, that is, over $\Delta\delta^{(0)}$ in relation (1.4), we expect the modulation by the magnetic flux to disappear, and with it all trace of coherent effects. The same kind of experiment was performed in 1981 by Sharvin and Sharvin [8] on a long hollow metallic cylinder threaded by an Aharonov–Bohm flux. A cylinder of height greater than L_ϕ can be interpreted as an ensemble of identical, uncorrelated rings of the type used in Webb's experiment. Thus, this experiment yields an ensemble average. Remarkably, they saw a signal which oscillated with flux but with a periodicity $\phi_0/2$ instead of ϕ_0. How can we understand that coherent effects can subsist *on average*?

The same type of question may be asked in the context of optics. If we average a speckle pattern over different realizations of disorder, does any trace of the phase coherence remain? Here too there was an unexpected result: the reflection coefficient of a wave in a turbid medium (sometimes called its albedo) was found to exhibit an angular dependence that could not be explained by the classical transport theory (Figure 1.8). This effect is known as *coherent backscattering*, and is a signature of phase coherence.

These results show that *even on average, some phase coherence effects remain*. In order to clarify the nature of these effects, let us consider an optically thick random medium. It can be modelled by an ensemble of point scatterers at positions $\boldsymbol{r}_n$ distributed randomly. The validity of this hypothesis for a realistic description of a random medium will be discussed in detail in Chapters 2 and 3. Consider a plane wave emanating from a coherent source (located outside the medium), which propagates in the medium and collides elastically with scatterers, and let us calculate the resulting interference pattern. For this, we study the complex amplitude $A(\boldsymbol{k}, \boldsymbol{k}')$ of the wave reemitted in the direction defined by the wave vector $\boldsymbol{k}'$, corresponding to an incident plane wave with wave vector $\boldsymbol{k}$. It may be written, without loss of generality, in the form

$$A(\boldsymbol{k}, \boldsymbol{k}') = \sum_{\boldsymbol{r}_1, \boldsymbol{r}_2} f(\boldsymbol{r}_1, \boldsymbol{r}_2)\, e^{i(\boldsymbol{k}\cdot\boldsymbol{r}_1 - \boldsymbol{k}'\cdot\boldsymbol{r}_2)}, \tag{1.5}$$

where $f(\boldsymbol{r}_1, \boldsymbol{r}_2)$ is the complex amplitude corresponding to the propagation between two scattering events located at $\boldsymbol{r}_1$ and $\boldsymbol{r}_2$. This amplitude may be expressed as a sum of the form $\sum_j a_j = \sum_j |a_j| e^{i\delta_j}$, where each path j represents a sequence of scatterings (Figure 1.9)

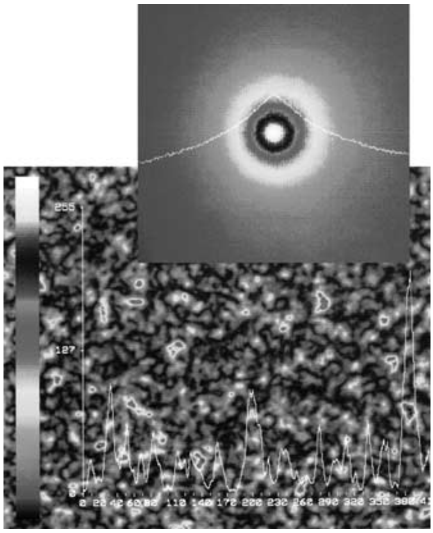

Figure 1.8 Speckle pattern obtained by multiple scattering of light by a sample of polystyrene spheres, as a function of observation angle. The curve in the lower figure represents the intensity fluctuations measured along a given angular direction. The upper figure is obtained by averaging over the positions of the spheres, and the resulting curve gives the angular dependence of the average intensity. (Figure courtesy of G. Maret.)

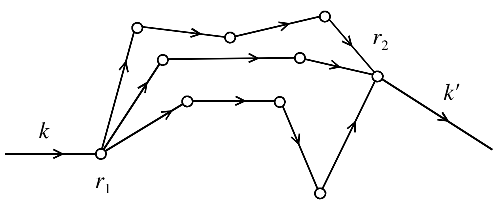

Figure 1.9 Typical trajectories which contribute to the total complex amplitude $f(\boldsymbol{r}_1, \boldsymbol{r}_2)$ of a multiply scattered wave.

joining the points $\boldsymbol{r}_1$ and $\boldsymbol{r}_2$. The associated intensity is given by

$$|A(\boldsymbol{k}, \boldsymbol{k}')|^2 = \sum_{\boldsymbol{r}_1, \boldsymbol{r}_2} \sum_{\boldsymbol{r}_3, \boldsymbol{r}_4} f(\boldsymbol{r}_1, \boldsymbol{r}_2) f^*(\boldsymbol{r}_3, \boldsymbol{r}_4)\, e^{i(\boldsymbol{k}\cdot\boldsymbol{r}_1 - \boldsymbol{k}'\cdot\boldsymbol{r}_2)}\, e^{-i(\boldsymbol{k}\cdot\boldsymbol{r}_3 - \boldsymbol{k}'\cdot\boldsymbol{r}_4)} \tag{1.6}$$

with

$$f(\boldsymbol{r}_1, \boldsymbol{r}_2) f^*(\boldsymbol{r}_3, \boldsymbol{r}_4) = \sum_{jj'} a_j(\boldsymbol{r}_1, \boldsymbol{r}_2)\, a^*_{j'}(\boldsymbol{r}_3, \boldsymbol{r}_4) = \sum_{jj'} |a_j||a_{j'}|\, e^{i(\delta_j - \delta_{j'})}. \tag{1.7}$$

In order to calculate its value averaged over the realizations of the random potential, that is, over the positions of scatterers, it is useful to note that most of the terms in relations (1.6)